Proceedings of ISFOG 2025
5TH INTERNATIONAL SYMPOSIUM ON
FRONTIERS IN OFFSHORE GEOTECHNICS
Nantes, France | June 9-13 2025

ISBN 978-2-85782-758-0

Skirt penetration in scour protection: laboratory and numerical analyses

R. Jahanshahi*
Universidad de Cantabria, Santander, Spain

D. Barreto
Edinburgh Napier University, Edinburgh, Scotland

M. Miranda, E. Rodriguez-Fernandez, J. Castro
Universidad de Cantabria, Santander, Spain

*mreza.jahanshahi@unican.es *(corresponding author)*

ABSTRACT: Skirts or shear keys are the most common elements used to provide sliding capacity to the foundation of post-piled offshore jackets prior to installation of the piles into the seabed. A protection system may be required to prevent scour, which can significantly affect the penetration of skirts and piles due to the grain size effect. Small-scale laboratory tests have been conducted to investigate the influence of grain size on the installation of skirts or the penetration of piles into two different granular materials using various plate thickness to grain size ratios ranging from 0.4 to 63. The results reveal that the plate penetration resistance increases with thicker skirts and higher soil friction angles as expected, but also as the grain size to plate thickness ratio is increased. To develop further knowledge of the effect of particle size on the penetration resistance of plates, discrete element modelling (DEM) is also utilized. Initially, triaxial tests were used to analyze the mechanical behaviour of the granular material modelled using DEM. Later, soil deposition of that granular material is simulated using periodic boundaries, and next, plate penetration is numerically modelled. Preliminary numerical results are presented, analyzed, and compared with the laboratory tests.

Keywords: Skirts; scour protection; grain size effect; penetration resistance; pile penetration.

1 INTRODUCTION

Wind energy is a highly efficient renewable resource, and the expansion of wind energy infrastructure has made the oceans a key area for wind energy generation.

One challenge in the construction of offshore wind farms is selecting the appropriate foundation, as it must account for varying water depths and seabed conditions, which can impact both the stability of the turbines and the overall cost and complexity of the project. Vertical steel elements must be driven into the seabed in some offshore foundations, for example in skirted, piled, or mudmat foundations (Feng et al., 2014; Varela et al., 2022, 2024). Thus, gaining insight into the penetration resistance of these types of steel elements is of great importance to ensure an efficient installation and is a subject that is currently being studied intensively due to its relevance (Cengiz et al., 2024).

Standards or recommended practices (API RP 2GEO 2011; DNVGL 2017) provide some guidance on the estimation of the penetration resistance through analytical or semi-empirical approaches, but some relevant aspects, such as the influence of the scour protection grain size or the interaction between penetrating elements are not considered. Further studies include Houlsby and Byrne (2005), who focused on analyzing the calculation methods suitable for the installation of caissons in sand. It was calculated that the resistance on both the inner and outer sides of the buckets or circular skirt plus the end bearing of the skirt for self-weight penetration. Additionally, Andersen et al. (2008) back-analyzed the penetration resistance of field tests, laboratory models, and prototypes in dense sand. They examined two existing approaches using either bearing capacity equations with friction angles obtained in laboratory tests or empirical correlations with CPT tip resistance. All proposed methods ignore the particle size effect on the penetration resistance. This can be assumed as long as the particle size is insignificant compared to the size of the penetrating element, such as in cohesive soils. However, coarse granular soils are typically used in scour protection systems and usually increase the penetration resistance as the grain size becomes comparable to the size of the penetrating elements.

The effect of grain size on cone resistance was studied by Bolton et al. (1999), Arroyo et al. (2011), and Lin and Wu (2012) using experimental tests and DEM modelling. It was found that a large grain size compared to cone diameter increases the penetration resistance and oscillations are observed due to the discontinuous granular flow. Most recently, Cerfontaine et al. (2023) studied the effect of grain size of granular materials on the penetration force of plain and rotary jacked piles. It was found that the response of open-ended piles is affected when the grain size is comparable to the wall thickness. Similar results were found in the work of Miyai et al. (2019), in which they concluded using DEM that the increase in the penetration force of vertical plates due to the grain size effect was related to the mobilization of a flow wedge with a width larger than the plate tip. This research was done from a fundamental granular matter perspective and the friction angle of the soil or bearing capacity equations were not considered.

Recently, the authors have studied this problem, analyzing the penetration resistance of steel plates in large field tests (Varela et al., 2022) and laboratory tests (Varela et al., 2024). Besides, these experimental results were successfully interpreted using a new approach, based on the equivalent plate thickness proposed by Miyai et al. (2019) and the bearing capacity equation, used for example, by Andersen et al. (2008).

This paper further analyses the laboratory study presented by Varela et al. (2024), as it is used as the reference case for DEM simulations of this problem. Finally, the preliminary results of the DEM simulations are presented.

2 MATERIALS AND EXPERIMENTAL METHODS

2.1 Test method

The penetration of steel plates of different thicknesses in sand and gravel was tested in the laboratory. Vertical pressure was applied to the plates to penetrate the rectangular plates into granular material. All plates had flat tips. The utilized granular material was kept in a methacrylate box having dimensions of 30 × 30 × 30 cm^3. A particular connector was used to secure the vertical alignment of the plates in the test. Vertical movement and vertical load of the plates were measured using a displacement transducer (LVDT) and load cells, respectively. The vertical force was applied at a steady rate of 4 mm/min, with the tests ending at a 100 mm displacement (penetration depth). However, results beyond 50 mm were influenced by the container's lateral boundaries and were not considered in the analysis.

The study aims to model how foundation elements like shear keys or steel plates penetrate loose granular soils (used for scour protection in offshore foundations). Therefore, the bulk unit weight of the soils was set to the lowest that could be achieved during the deposit-filling process. The tests used dry sand and gravel to replicate drained conditions similar to real-world scenarios, though the dry unit weight differed from the submerged saturated unit weight. Despite this difference, the results can validate theoretical models.

The deposited sand and gravel were poured in five uniform layers, each approximately 4.4 cm thick, using a funnel and tube to ensure consistent deposition. The container was filled up to 22 cm of soil, resulting in a total volume of 0.016 m³. Further details of the test procedure can be found in Varela et al. (2024).

2.2 Materials

The study used two soils for testing: sand from Los Peligros beach (Santander, Spain), which contained shell fragments and had a uniform grain size, and crushed limestone gravel. Both soils had minimal fine particles, making them frictional with no cohesion. Mechanical properties, particularly friction angles, were determined through drained triaxial and direct shear tests, conducted at the same densities as those for the penetration tests. Further details of these tests are available in Varela et al. (2024).

Five plate thicknesses (1, 2, 5, 10, and 20 mm) were tested. All plates were 115 mm x 190 mm with attachment holes, made of steel except the 1 mm which is a tin plate. They had flat, rectangular tips. Table 1 shows the ratio between the plate tip thickness and d_{50} of the granular materials used in this study.

Table 1. Ratio between plate thickness (t) and mean grain size (d_{50})

Thickness	**Gravel (d_{50} = 2.43 mm)**	**Sand (d_{50} = 0.32 mm)**
t (mm)	**t/ d_{50} ratio - gravel**	**t/ d_{50} ratio - sand**
1	0.4	3
2	0.8	6
5	2	16
10	4	31
20	8	63

3 RESULTS AND DISCUSSION

3.1 Laboratory test and theoretical method

Figure 1 shows penetration stress (s) vs. penetration depth (z) measured in gravel. For calculating the penetration stress, using the equivalent plate thickness ($t_{eq} = t + d_{50}$) proposed by Miyai et al. (2019). As seen, the penetration stress is in the same range for all plates at lower penetration depth. The difference in deeper depth could be because of the boundary effects of the used box in the tests, especially for thicker plates (Varela et al. 2024). Additional cases of plate penetration in the sand can be found in Varela et al. (2024). Despite slight differences in the initial unit weight, reasonable repeatability of the results was observed for each case. For example, the test with the highest unit weight in gravel (red lines in Figure 1) also showed the highest penetration stress. Oscillations in the load, attributed to granular flow around the penetrating tip, were more noticeable in gravel due to the larger grain size and were influenced by the plate thickness.

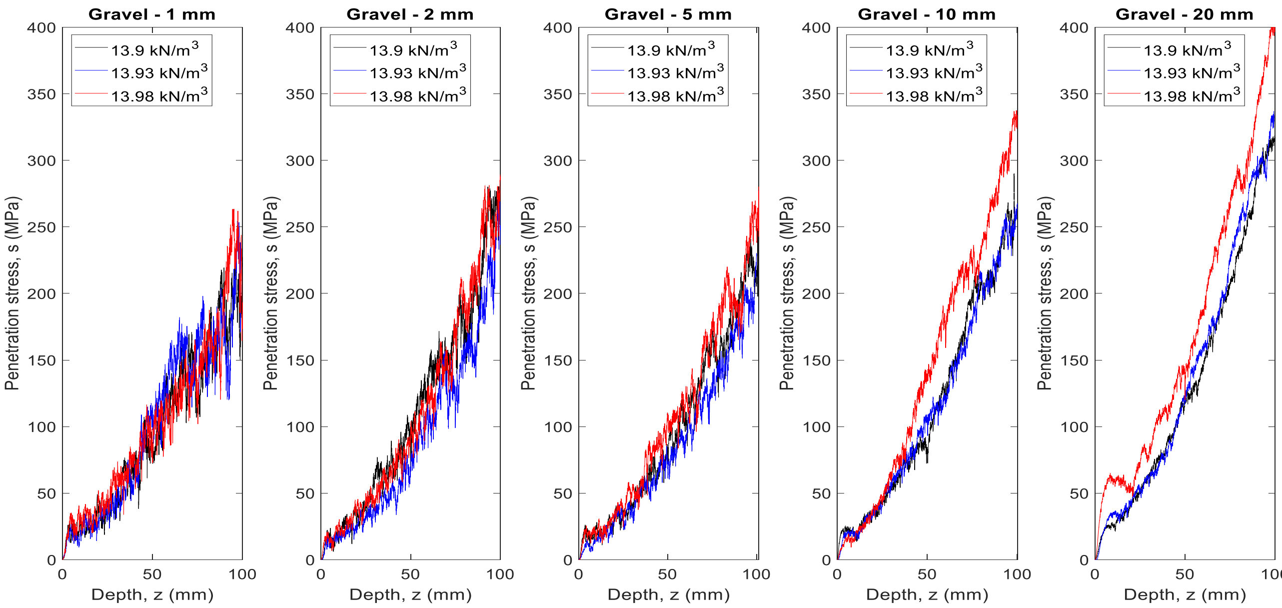

Figure 1. Penetration stress results from different plates into gravel using the equivalent plate thickness

In this study, the penetration force (R) was divided by the length of the plate (L) to show the penetration force per unit length. As seen in Figure 2, the load-displacement curves can be divided into three parts through a closer visual analysis of the curves. Part 1 shows a rapid, linear load increase as the plate first contacts the soil, the soil initially deforms elastically, quickly leading to soil yielding and formation of the full plastic mechanism (Feng et al., 2019). This phase usually ends when the plate has penetrated almost 1-3 mm into the sand. Part 2 features a linear load increase with penetration due to the evolution with depth of the full plastic mechanism and to the minimal wall friction influence. In Part 3 a slight curvature is observed due to the influence of the walls' friction on the penetration load. The boundaries between these phases are defined by load-displacement analysis, with the transition points depending on plate thickness and soil type.

A linear fitting was proposed to distinguish between part 2 and part 3 in the penetration curves. This fitting was chosen between 10-20 mm of penetration depth in sand. As shown in Figure 2, When the load value consistently exceeds 5% of the value estimated by the linear adjustment, the start of part 3 of the curve was set.

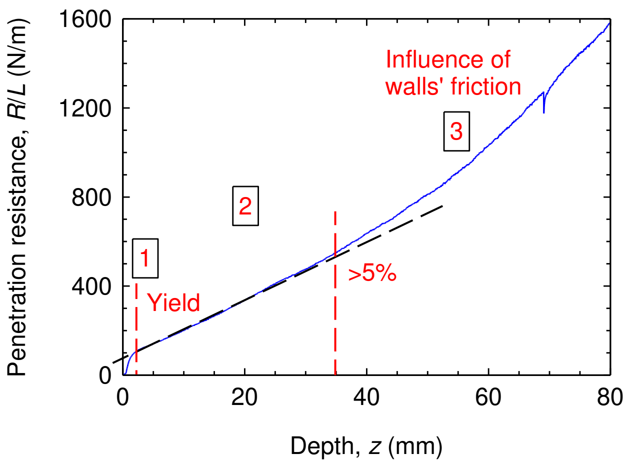

Figure 2. Different behaviours of the 20-mm-thick plate during penetration in sand.

The analytical approach used here to back-calculate the friction angle using the penetration results of the laboratory tests is based on Andersen et al. (2008), using the equivalent approach proposed by Miyai et al. (2019), as shown in Varela et al. (2022, 2024).

These calculated values are then compared with measured friction angles obtained from direct shear and triaxial tests (Varela et al., 2024). Table 2 compares the average values of the friction angle measured in the laboratory with the average of the back-calculated friction angles considering the real plate thickness (t) or different equivalent plate thicknesses (t_{eq}). It is worth noting that the friction angles measured in the laboratory notably vary with the confining stress or the normal stress. The back-calculated values using equivalent plate thicknesses are more consistent and, as can be seen in Table 2, they agree better with the triaxial test results. Also, the new equivalent thickness proposed by Varela et al. (2024), using d_{99}, improved the theoretical interpretation with more consistent soil friction angles compared to the one using d_{50}.

Table 2. Comparison between mean back-calculated friction angles from penetration tests and those measured using triaxial direct shear tests.

Soil type	t	t+d₅₀	t+d₉₉	Triaxial	Direct shear
Sand	41°	40°	39°	37°	48°
Gravel	49°	45°	45°	43°	62°

3.2 Discrete element modelling

In this section, discrete element modelling (DEM) was used and the previous laboratory tests were used as a reference case. However, at this moment, the laboratory results and simulations are not meant to be compared. The free code YADE (Smilauer et al., 2015) was used. Initially, triaxial tests were numerically simulated to analyze the mechanical behaviour of the granular materials. For both model generation and triaxial test simulation, the inter-particle friction angle of soil was set at 16.70° (μ = 0.3), first to generate a loose sample under different isotropic pressures of 50 kPa, 150 kPa, and 300 kPa and then to properly reproduce the inter-particle friction.

Table 3. Properties used for the DEM simulations.

Parameters	*Value*	Unit
Particle density (ρ)	2600	kg/m^3
Normal contact stiffness (k_n)	1×10^6	N/m
Shear contact stiffness (k_s)	1×10^6	N/m
Initial inter-particle friction angle ($\phi_{\mu o}$)	16.70	°
Inter-particle friction angle (ϕ_μ)	16.70	°
Particle size distribution (PSD)	1-2	mm

The contractive behaviour of the sample can be tracked using the deviatoric stress vs. axial strain response and volumetric deformation curves, as seen in Figure 3. As expected, the DEM sample of the soil experienced higher values of deviatoric stress as the isotropic stress increased from 50 kPa to 300 kPa. From these triaxial test simulations, a friction angle of around 19° may be interpreted. This was lower than the value obtained from the laboratory test, as only spherical particles were considered in DEM at this stage.

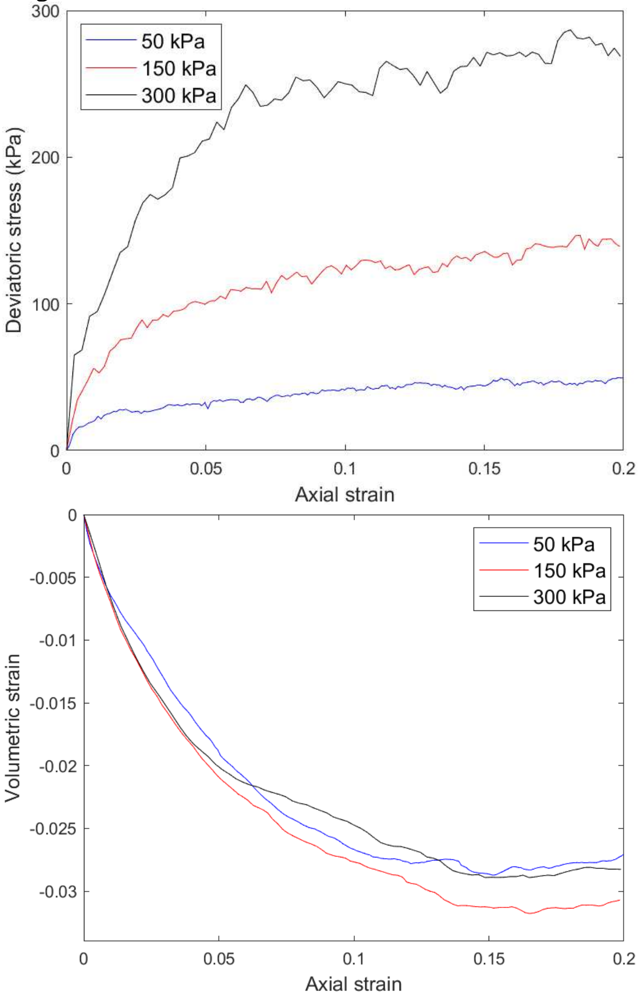

Figure 3. Response of the loose DEM sample to shearing

To simulate the penetration of a plate into the soil, a 270 mm wide box was considered. As the studied penetration problem is under plain-strain conditions, periodic boundaries were utilized to determine the thickness of the box and it was initially set to 25 mm. After finishing the deposition of the particles inside the box with the properties shown in Table 3, a plate was simulated and pushed into the soil with a vertical velocity of 200 mm/min. The particle size distribution of the models was set to 1-2 mm with percentages ranging from 0 to 100%. Therefore, the d_{50} of this soil sample is 1.5 mm. All tests were stopped once the plate tip reached a depth of 70 mm from the top surface of the model. All numerical simulations were conducted within a three-dimensional framework.

Sensitivity analyses of the width (W) and thickness (distance between periodic boundaries, P) of the box were performed to minimize the number of particles used in numerical modelling. This also needs to ensure that reducing the size of the boundaries does not affect the response of the plate penetration in the numerical model. Also, the largest thickness of the plate from those used in the laboratory tests (namely t =20 mm) is initially being used. Figure 4 shows the schematic view of the model in this study.

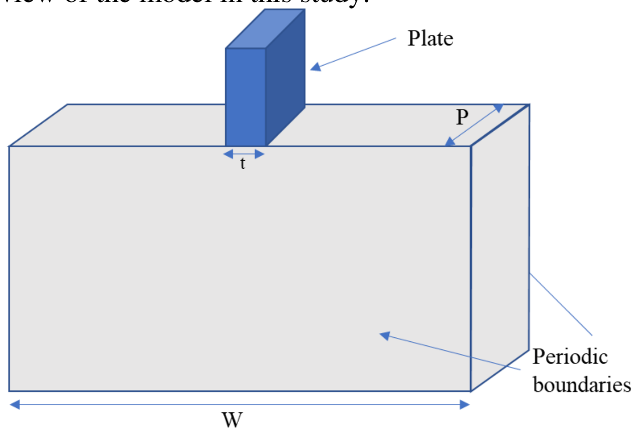

Figure 4. Schematic view of the models

A summary of the effect of the boundary size on the response of the plate penetration in the soil is shown in Figure 5. As previously observed by Andersen et al. (2008), Miyai et al. (2019), Miranda et al. (2024), and Varela et al. (2022, 2024), the tip resistance component of the penetration force is the highest and the frictional resistance component is mostly negligible. Therefore, in this graph, only the tip component was considered to study boundary effects. As seen in Figure 5, the penetration force is affected by the width of the model when it is less than 200 mm. Therefore, selecting a width greater than or equal to 200 mm is expected to reduce the influence of the side boundaries on the plate's response to penetration. To analyse in more detail, fitting lines were proposed for the penetration curves obtained using DEM analysis between 10 mm to 50 mm penetration depths. As seen in Table 4, the difference between the slopes becomes more than 10% when the model's width falls below 200 mm.

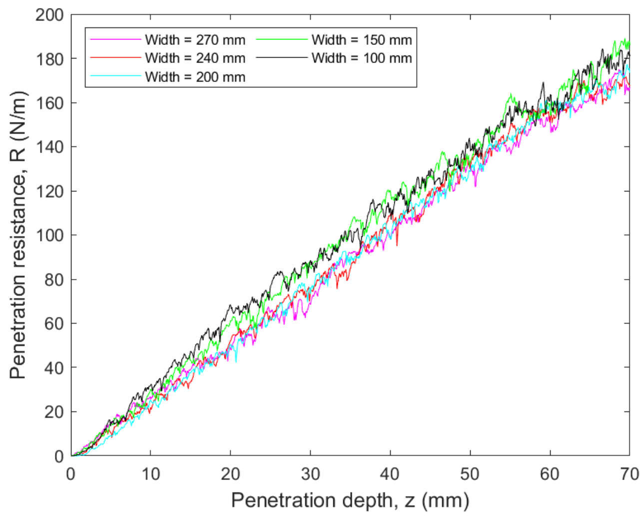

Figure 5. Effect of the width of the model on the penetration response for models with a thickness of 25 mm

To evaluate the effect of the distance between the front and back periodic boundaries on the penetration force, the initial thickness of the box was also reduced. The obtained penetration force was divided by the box thickness to evaluate the influence of the thickness of the periodic boundary on the penetration force. As seen in Figure 6, any box thickness equal to or greater than 35 mm is supposed to have a negligible effect on plate penetration response.

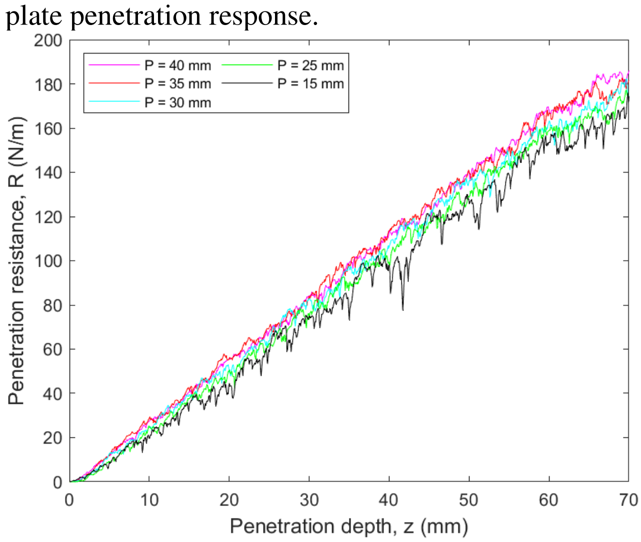

Figure 6. Effect of the thickness of the model (periodic boundary size) on the penetration response for models with a width of 200 mm

Table 4. The slope of the fitting lines of the response of the plate penetration in numerical models

Width (mm)	Slope	Periodic boundaries' distance (mm)	Slope
270	2.53	40	2.79
240	2.58	35	2.78
200	2.57	30	2.68
150	2.84	25	2.57
100	2.86	15	2.45

4 CONCLUSION

Laboratory tests were conducted to study the effect of grain size on skirt penetration in granular soils using five steel plate thicknesses in sand and gravel, with plate thickness to grain size ratios between 0.4 and 63. Thirty penetration tests as well as triaxial and direct shear tests were performed to characterize soil friction angle. It was found that the penetration resistance depends on plate thickness, soil friction angle, and grain size. The authors' new approach for estimating the static penetration resistance in scour protection systems (Varela et al. 2022, 2024) was validated across a wider range of tests based on existing analytical bearing capacity equations and an equivalent thickness.

Preliminary results of DEM simulations have been presented to gain knowledge of the plate penetration problem further. The boundary effect of the numerical models was studied, and it was shown that a model with a periodic boundary distance of 35 mm and a width of 200 mm did not affect the plate penetration results.

AUTHOR CONTRIBUTION STATEMENT

R. Jahanshahi: Conceptualization, Methodology, Investigation, Data curation, Visualization, Writing - Original Draft. **D. Barreto**: Validation, Conceptualization, Methodology, Investigation, Supervision. **M. Miranda**: Conceptualization, Methodology, Supervision, Writing - Review & Editing, Funding acquisition. **E. Rodriguez-Fernandez**: Validation, Methodology, Investigation. **J. Castro**: Conceptualization, Methodology, Supervision, Writing - Review & Editing, Funding acquisition.

ACKNOWLEDGMENT

The authors acknowledge financial support from the Spanish Ministry of Economic Affairs and Digital Transformation (MINECO) and the European Regional Development Fund (ERDF) for the project "Foundation of Offshore Platforms for Renewable Energies" (PEJ2018-003335-A), funded by the Youth Employment Initiative (YEI) and European Social Fund (ESF). This work is also part of the ThinkInAzul program, supported by the Ministerio de Ciencia e Innovación (PRTR-C17.I1), Comunidad Autónoma de Cantabria, and the project "Advanced Methodology for Foundation of Critical Structures in Offshore Wind Farms" (TED2021-130780B-I00), funded by MICIU/AEI and the European Union NextGenerationEU/PRTR.

REFERENCES

Andersen, K.H., Jostad, H.P. and Dyvik, R. (2008). Penetration resistance of offshore skirted foundations and anchors in dense sand. *Journal of Geotechnical and Geoenvironmental Engineering*, 134(1): 106–116. http://doi.org/10.1061/(ASCE)1090-0241(2008)134:1(106).

API (American Petroleum Institute). (2011). Petroleum and natural gas industries—Specific requirements for offshore structures. In Part 4—Geotechnical and foundation design considerations (API RP 2GEO). Washington, DC: API.

Arroyo, M. et al. (2011). Cone penetration tests in a virtual calibration chamber. *Geotechnique*, 61(6): 525–531. http://doi.org/10.1680/geot.9.P.067.

Bolton, M.D. et al. (1999). Centrifuge cone penetration tests in sand. *Géotechnique*, 49(4): 543–552. http://doi.org/10.1680/geot.1999.49.4.543.

Cengiz, C., et al. (2024). Optimising pile installation through scour protection (OPIS) project and preliminary findings. In Proceedings of the 5th European Conference on Physical Modelling in Geotechnics (ECPMG 2024), pp. 1–8.

Cerfontaine, B. et al. (2023). DEM study of particle scale effect on plain and rotary jacked pile behaviour in granular materials. *Computers and Geotechnics*, 161: 105559. http://doi.org/10.1016/j.compgeo.2023.105559.

DNVGL. (2017). Offshore soil mechanics and geotechnical engineering (DNVGL-RP-C212). Bærum, Norway: DNVGL.

Feng, X. et al. (2014). Design approach for rectangular mudmats under fully three-dimensional loading. *Geotechnique*, 64(1): 51–63. http://doi.org/10.1680/geot.13.P.051.

Feng, Y., Blumenfeld, R. and Liu, C. (2019). Support of modified Archimedes' law theory in granular media. *Soft Matter*, 15(14): 3008–3017. http://doi.org/10.1039/c8sm02480d.

Houlsby, G.T. and Byrne, B.W. (2005). Design procedures for installation of suction caissons in sand. *Proceedings of the Institution of Civil Engineers - Geotechnical Engineering*, 158(3): 135–144. http://doi.org/10.1680/geng.2005.158.3.135.

Lin, J. and Wu, W. (2012). Numerical study of miniature penetrometer in granular material by discrete element method. *Philosophical Magazine*, 92(28–30): 3474–3482. http://doi.org/10.1080/14786435.2012.706373.

Miranda, M. et al. (2024). Experimental tests to evaluate skirt penetration resistance in scour protection for offshore foundations, in *Proceedings of the XVIII ECSMGE 2024*, pp. 3145–3148. http://doi.org/10.1201/9781003431749-618.

Miyai, S. et al. (2019) 'Influence of particle size on vertical plate penetration into dense cohesionless granular materials (large-scale DEM simulation using real particle size)', *Granular Matter*, 21(4): 105. http://doi.org/10.1007/s10035-019-0961-z.

Smilauer, V. et al. (2015). Yade documentation. *Yade documentation* (2nd ed.) [Preprint]. http://doi.org/10.5281/zenodo.5705394.

Varela, E. et al. (2022). Full-scale tests of skirt penetration resistance in gravel for offshore wind structures. *Journal of Geotechnical and Geoenvironmental Engineering*, 148(11): 04022084. http://doi.org/10.1061/(asce)gt.1943-5606.0002889.

Varela, E., Miranda, M. and Castro, J. (2024). Laboratory tests of skirt penetration in loose granular soils. *Marine Georesources & Geotechnology*. http://doi.org/10.1080/1064119X.2024.2348635.